



## Diclofenac enhances Boron nitride nanoparticle toxicity in freshwater green microalgae, *Scenedesmus obliquus*: Elucidating the role of oxidative stress

Soupam Das<sup>a</sup>, Shinta Ann Jose<sup>a</sup>, Sampriti Giri<sup>a</sup>, Janmey Shah<sup>a</sup>, Mrudula Pulimi<sup>a</sup>, Shalini Anand<sup>b</sup>, Pramod Kumar Rai<sup>b</sup>, Amitava Mukherjee<sup>a,\*</sup>

<sup>a</sup> Centre for Nanobiotechnology, Vellore Institute of Technology, Vellore, Tamil Nadu, India

<sup>b</sup> Centre for Fire, Explosives and Environment Safety, Timarpur, Delhi 110054, India

### ARTICLE INFO

Handling Editor: Prof. L.H. Lash

#### Keywords:

NSAID  
Ecotoxicity  
ROS  
Photosynthetic efficiency  
Lipid peroxidation

### ABSTRACT

Boron nanoparticles have numerous medical, industrial, and environmental applications as potential nanomaterials. Given the inevitable release of these particles in aquatic environments, they can combine with other pollutants like pharmaceuticals. Therefore, it is necessary to investigate their combined detrimental effects on freshwater biota. This study examined the joint impacts of Boron nitride nanoparticles (BNNPs) and Diclofenac (DCF) on freshwater microalgae *Scenedesmus obliquus*. Three different concentrations of BNNPs (0.1, 1, and 10 mg L<sup>-1</sup>) were mixed with 1 mg L<sup>-1</sup> of DCF and were treated with algal cells, and biochemical analyses were performed. A concentration-dependent decrease in algal cell viability was observed after a 72-h interaction period with BNNPs and their binary combinations. The maximum toxic effects were observed for the highest combination of BNNPs + DCF, i.e., 10 mg L<sup>-1</sup> BNNPs + 1 mg L<sup>-1</sup> DCF. Similarly, an increase in the oxidative stress parameters and antioxidant enzyme activity was observed, which correlated directly to the decline in cell viability. The algal cells also showed reduced photosynthetic efficiency and electron transfer rate upon interaction with BNNPs. The results of this research emphasize the importance of considering the negative consequences of emerging pollutants and their combinations with other pollutants, BNNPs, and DCF as part of a thorough evaluation of ecotoxicity in freshwater algal species.

### 1. Introduction

Diclofenac (DCF) is a medication that falls under the category of non-steroidal anti-inflammatory drugs (NSAIDs) [39]. It is known for its notable antirheumatic, anti-inflammatory, analgesic, and antipyretic properties [32]. Over the past few years, there has been a significant rise in the global production and consumption of diclofenac, reaching an estimated 940 tons per year. It is available in various forms, such as capsules, ointments, and intravenous solutions [44]. DCF undergoes hepatic detoxification through hydroxylation and glucuronidation following administration. A significant portion of the oxidized metabolites are eliminated through the kidneys, while the remaining portion is excreted in the bile as acyl glucuronide. Some diclofenac remains unchanged and is not broken down in the body. As a result, it can end up in the sewage system at concentrations of several hundred µg L<sup>-1</sup> [39]. According to a study by Sathishkumar et al. [40], it has been found that traditional sewage treatment plants, which use limited physico-chemical

methods, are not very effective in completely removing DCF residues that are commonly present in freshwater systems. Despite the various transformations that occur in the environment, DCF can be found in its original form at concentrations ranging from a few ng L<sup>-1</sup> to tens of mg L<sup>-1</sup> [1,32,39,40]. In a recent study by Sathishkumar et al. [40], the researchers highlighted the negative impacts of DCF on various organisms, ranging from microalgae to large fishes and, ultimately, to mammals. Several studies have documented the acute toxicity of DCF in various aquatic organisms, including fish, prawns, copepods, mussels, and crustaceans [18,2,26,31,43].

Boron nitride nanoparticles (BNNPs) have garnered significant attention over the past few years owing to their numerous advantages, such as superior thermal stability, compared to other carbon-based nanomaterials [34]. Applications for boron nanoparticles include drug delivery, tissue engineering, bioimaging, optoelectronics, photocatalysis instruments, sensor devices, and storing energy [19,25,47]. The increase in the production and utilization of BNNPs would result in their

\* Correspondence to: Centre for Nanobiotechnology Vellore Institute of Technology, Vellore 632014, India.

E-mail addresses: [amit.mookerjee@gmail.com](mailto:amit.mookerjee@gmail.com), [amitav@vit.ac.in](mailto:amitav@vit.ac.in) (A. Mukherjee).

<https://doi.org/10.1016/j.toxrep.2024.101696>

Received 2 June 2024; Received in revised form 6 July 2024; Accepted 12 July 2024

Available online 14 July 2024

2214-7500/© 2024 The Author(s). Published by Elsevier B.V. This is an open access article under the CC BY-NC license (<http://creativecommons.org/licenses/by-nc/4.0/>).

unregulated discharge into freshwater ecosystems, posing a threat to the subaqueous flora and fauna. Concerns have been raised about the accumulation of these nanomaterials in freshwater bodies. The photocatalytic nature and the bio persistence of BNNPs also pose a severe threat to freshwater organisms [41].

Microalgae are essential in generating biomass and contributing to the fundamental nutrition of aquatic systems. Additionally, it serves as a critical marker of water pollution. *Scenedesmus obliquus* is a commonly utilized microalgal species for research due to its rapid growth rate, uncomplicated cell cycle, and similar photosynthetic and metabolism processes to higher plants. Furthermore, it was observed that *Scenedesmus* sp. exhibited greater sensitivity compared to other freshwater microalgae, such as *Chlorella* sp., that were present in our laboratory [10]. Saxena et al. [41] conducted a toxicity test with nano and bulk forms of BNNPs on different freshwater microalgal cells, *Chlorella vulgaris*, and *Coelastrella terrestris* at 10, 25, and 50 mg L<sup>-1</sup> concentrations. They observed reduced growth rates and increased malondialdehyde production of the algal cells when interacting with the nanoparticles. Furthermore, they also found that the nano form of boron nitride was more toxic than its bulk form. One drawback of this study is that they did not observe the toxic effects of boron nitride nanoparticles at lower concentrations. Another study by Dağlıoğlu and Öztürk [9] found reduced cell viability and chlorophyll content of freshwater microalgae *Chodatodesmus mucronulatus* when interacted with nano boron for 24, 48, and 72 h at a concentration of 50 mg L<sup>-1</sup>. They also did not observe the toxic effects of the nanoparticles at various other concentrations. A study by Doležalová Weissmannová et al. [14] showed adverse effects of DCF when interacted with *Desmodesmus subspicatus*. The toxicity of DCF was further enhanced when cadmium was combined with it. Another study by Cleuvers [8] observed that DCF has significant toxic effects on freshwater microalgae *D. subspicatus* and *Daphnia*. They also reported that DCF has no particular mode of action for causing its toxic effects.

Upon critical examination of prior research on boron nanoparticles and diclofenac, it is evident that there needs to be a more comprehensive exploration regarding its effects on freshwater microalgae. Furthermore, the potential role of reactive oxygen species generation in toxicity still needs to be addressed in the existing literature. Contrary to the previous study, in the current study, the freshwater microalgae *S. obliquus* was exposed to three different, environmentally relevant concentrations of BNNPs and one concentration of DCF. The methodology for this study was developed to emulate real-world exposure conditions. Following our previous studies, we utilized filtered and sterilized natural freshwater as the exposure medium [37]. After interacting *Scenedesmus obliquus* with BNNPs + DCF and their pristine counterparts, the experimental design included the cell viability assay, quantifying the formation of reactive oxygen species, and assessing the antioxidant enzyme activities. In addition to that, photosynthetic efficiency and electron transport rate were also observed.

## 2. Materials and methods

### 2.1. Materials used

The boron nitride nanoparticles (BNNPs) procured from the DRDO-CFEES lab, Centre for Fire, Explosives and Environment Safety (Timarpur, Delhi 110054, India) were used for this study. Other chemicals, such as Diclofenac (DCF), 2',7'-dichlorofluorescein diacetate (DCFH-DA), were supplied from Sigma Aldrich. Aminophenyl fluorescein (APF) and Dihydroethidium (DHE) were obtained from Invitrogen TM, Molecular Probes®, CA, USA. Hydroxylamine hydrochloride, Thiobarbituric acid (TBA), trichloroacetic acid (TCA), BG-11 medium, and dimethyl sulfoxide (DMSO) were supplied from Hi-Media Pvt. Ltd (Mumbai, India). Nitroblue tetrazolium chloride (NBT) and Hydrogen Peroxide solution (H<sub>2</sub>O<sub>2</sub>- 30 % w/v) were bought from SDFCL, Mumbai, India.

### 2.2. Isolation and maintenance of culture

The algal species *Scenedesmus obliquus* isolated from the VIT Lake, Vellore (12°58'10" N, 79°9' 37" E), was used as the model organism in the present study. The subcultures were maintained in a sterilized BG-11 medium. The growing cultures were exposed to a white fluorescent illumination of 3000 lx (Philips TL-D Super 80, linear fluorescent lamp, India) for a photoperiod of 16 h at 23 ± 2 °C in a chamber with temperature control (I.L.E. Co., India) [36].

### 2.3. Lakewater Collection and filtration

The current study used freshwater as the interaction matrix to emulate the environmental conditions [11]. This freshwater was collected from the Lake inside the VIT campus, Vellore (Tamil Nadu, India), and was processed through filtration. Initially blotting paper was used to eliminate the larger debris, followed by the Whatman no.1 filter paper (pore size 11 µm) to eliminate all other colloidal particles. Finally, the filtrate was sterilized in an autoclave at 121 °C for 15 min. This freshwater medium was utilized throughout the study to perform all the experiments [37].

### 2.4. Preparation of BNNPs, DCF stock solutions, and working concentrations

The BNNPs were dispersed in deionized water to prepare a concentrated stock solution. The nanoparticles were ultrasonicated for 30 mins in a 130 W (20 kHz) ultrasonic processor (Sonics, USA) to achieve even dispersion. Ecotoxicological studies require accurately estimating toxic substances' Effective Concentration (EC<sub>x</sub>) (OECD 201, 2002). The algal-specific growth rate inhibition was determined with the EC<sub>x</sub> values EC<sub>10</sub>, EC<sub>50</sub>, and EC<sub>90</sub>. These EC values represent the concentration of BNNPs resulting in 10, 50, and 90 % algal inhibition. The working concentration for the study was selected after analyzing the EC<sub>50</sub> values for the BNNPs. The EC<sub>x</sub> values were calculated using the EPA probit analysis. The required volumes of the aliquots were taken from the stock solution to obtain the desired working concentrations of 0.1, 1, and 10 mg L<sup>-1</sup>. The stock solution of DCF was prepared freshly by mixing 100 mg/L of DCF in Milli-Q water. The working concentration of the DCF was selected after analyzing the EC<sub>50</sub> values. One concentration below the EC<sub>50</sub> value was determined to be the working concentration of DCF, i.e., 1 mg L<sup>-1</sup>.

### 2.5. Characterization of BNNPs and its combination with DCF

The surface topography of the BNNP suspensions was analyzed using a high-resolution field emission scanning electron microscope (FE-SEM) (Thermo Fisher FEI Quanta 250 FEG). The X-ray diffractometer (Advanced D8, Bruker, Germany) assessed the purity and crystallinity of Boron nitride nanoparticles. Fourier Transform Infrared Spectroscopy (FTIR) was performed to confirm the primary functional group in the sample. Further, the charge on the pristine BNNPs and BNNPs + DCF combined in lake water was determined by Zeta Potential. The DLS (90 Plus Particle Size Analyzer, Brookhaven Instruments Corp., USA) was used to measure the mean hydrodynamic diameter (MHD) of the particles in lake water at both the 0th and 72nd h to study the aggregation and distribution patterns of the particles.

### 2.6. Microalgal interaction with BNNPs

The interaction studies were conducted with the microalgae grown up to the late log phase. The pellet from the centrifuged algal culture was made up to an optical density of 0.5. The desired working concentrations, 0.1, 1, and 10 mg L<sup>-1</sup> of pristine BNNP suspension, 1 mg L<sup>-1</sup> of pristine DCF, and their combinations (0.1 mg L<sup>-1</sup> BNNPs + 1 mg L<sup>-1</sup> DCF; 1 mg L<sup>-1</sup> BNNPs + 1 mg L<sup>-1</sup> DCF; and 10 mg L<sup>-1</sup> BNNPs +

1 mg L<sup>-1</sup> DCF), were prepared by adding the necessary volume of aliquots from the stock suspension into the algal culture. The interaction mixture with the algal culture and sample suspension comprised a total volume of 5 mL with the filtered, sterilized lake water. Further, this mixture was kept for 72-h interaction under visible light conditions at 23 °C by following the OECD guidelines Test No. 201 [29]. A set of interaction mixtures without the nanoparticle sample was kept as the control for the experiment. All the investigations in this study were conducted in triplicates (n=3) to obtain and validate the statistical significance of the findings.

## 2.7. Cell enumeration

An aliquot of 20 µL from the interacted algal samples (both control and test) was placed on a hemocytometer and examined using a light microscope (Zeiss AxioStar Microscope, USA). The growth inhibition of *Scenedesmus obliquus* was determined by counting the healthy algal cells and comparing the counts with the control algal cells.

## 2.8. Analysis of oxidative stress

### 2.8.1. Overall ROS generation

The intracellular ROS production was measured in the 72 h interacted samples using DCFH-DA (ROS indicator), a cell-permeable fluorescent dye. The protocol can be followed from [12]. The detailed methodology has been mentioned in Method S1 of the [supplementary information](#).

### 2.8.2. Superoxide and hydroxyl radical generation

Superoxide radicals in the interacted algal samples were assessed using the freely permeable blue fluorescent dye, Dihydroethidium (DHE), which reacts with the superoxide generated within the cells and forms red fluorescent ethidium. The procedure followed by [30] was used for the analysis. The complete methodology has been detailed in the supplementary file under Method S2.

APF (Aminophenyl fluorescein) dye was used to assess the production of hydroxyl radicals in algal cells. The experiment protocol was followed by [13]. The detailed methodology has been explained in the supplementary file under Method S3.

### 2.8.3. Lipid peroxidation

Lipid peroxidation involves reactive oxygen species damaging lipids, especially polyunsaturated fatty acids, in the cell membranes of microalgae. The measurement focuses on Malondialdehyde (MDA), a recognized by-product of microalgae under stress. The protocol to perform this assay has been mentioned in one previous study [33]. The complete methodology is given in the supplementary file under Method S4.

## 2.9. Antioxidant enzyme assay

### 2.9.1. Superoxide dismutase (SOD) Activity

Superoxide dismutase assay for the treated cells was performed by the protocol described by [28]. The detailed methodology has been mentioned in supplementary file under Method S5.

### 2.9.2. Catalase activity

Determining catalase enzyme activity in *Scenedesmus obliquus* was conducted following the protocol outlined by Chakraborty et al. [3]. The detailed protocol is written in supplementary file under Method S6.

## 2.10. Photosynthetic efficiency of PS II and electron transport rate (ETR)

The protocol for analyzing photosynthetic efficiency is mentioned elsewhere [17]. The complete methodology has been outlined in [supplementary information](#) (Method S7).

Similarly, the [supplementary information](#) details the methodology

for analyzing the electron transport rate (Method S8). This protocol has been followed from Romanowska-Duda et al. [35].

## 2.11. Statistical analysis

All the experiments were performed in triplicates (n=3). The statistical difference between the control and the samples was achieved using two-way ANOVA with Bonferroni's multiple comparison tests in Graph Pad Prism 8. The accepted significance level was  $p < 0.05$ ; the data were represented as mean  $\pm$  SD (Standard Deviation).

The interactions between two particles in a mixture were analyzed using the Independent Action Model (Abbott, 1925). The goal was to determine whether these interactions were synergistic, antagonistic, or additive. This model is commonly used to assess the effects of contaminants compared with normal mortality rates. This method proves to be highly effective for mixtures containing only two particles. The detailed methodology has been provided in the supplementary file under Method S9.

## 3. Results

### 3.1. Characterization and colloidal stability analysis of the nanoparticles

FE-SEM images were used to identify the shapes, sizes, and morphology of BNNPs. FE-SEM images (Fig. 1A) indicated that BNNPs were uniform, regular, and almost polymorphic shapes with smooth surfaces; the average size was estimated to be approximately 262 nm.

Fig. 1B represents the FTIR spectra of BNNPs. The peaks at 3206 cm<sup>-1</sup>, 2261 cm<sup>-1</sup>, 1415 cm<sup>-1</sup>, and 1186 cm<sup>-1</sup> are attributed to stretching vibrations of B-OH, C≡N, BN, and BN-O. The peaks at 717 cm<sup>-1</sup> and 640 cm<sup>-1</sup> represent B-N and C=C bending vibrations. The FTIR spectra confirm the presence of boron nitride (Singh et al., 2016).

The mean hydrodynamic diameter of BNNPs at 0th h in lake water medium was found to be 191.05  $\pm$  8.29, 442.28  $\pm$  2.71, and 603.65  $\pm$  1.32 nm for 0.1, 1, and 10 mg L<sup>-1</sup>, respectively. Table S1 summarizes the changes in the mean hydrodynamic diameters of the various concentrations of BNNPs and their combination with DCF in lake water medium at 0th and 72 h time intervals. The zeta potential values for pristine BNNPs and BNNPs + DCF combinations are represented in Table S2. X-ray diffraction (XRD) analysis was additionally conducted, revealing the presence of a boron nitride peak. (Fig S1).

### 3.2. Analysis of growth inhibition

The EC<sub>10</sub>, EC<sub>50</sub>, and EC<sub>90</sub> values of BNNPs interacted with *Scenedesmus obliquus* in lake water medium were observed to be 0.01, 4.72, and 1318 mg L<sup>-1</sup>, respectively. The EC<sub>50</sub> value for DCF is 2 mg L<sup>-1</sup>. *S. obliquus* cells treated with different concentrations (0.1, 1, and 10 mg L<sup>-1</sup>) of BNNPs decreased in cell growth, where significant differences were noted in compared to control ( $p < 0.001$ ) (Fig. 2). The algal cells treated with different concentrations of binary mixture showed further reduction in cell growth which is significant in comparison to untreated cells and pristine BNNPs treated cells ( $p < 0.001$ ).

An independent action modeling was performed to describe the interaction between BNNPs and DCF after exposure (Table 1). The RI value decreased as the BNNP concentration increased, which was found to be statistically significant. This confirms an antagonistic interaction for all combinations.

### 3.3. Oxidative stress generation

Fig. 3A represents the total ROS generated when the *S. obliquus* cells are exposed to pristine DCF, various concentrations of BNNPs, and BNNPs + DCF combination. In particular, in the presence of 0.1, 1, and 10 mg L<sup>-1</sup> BNNPs, the total ROS levels of the exposed cells increased

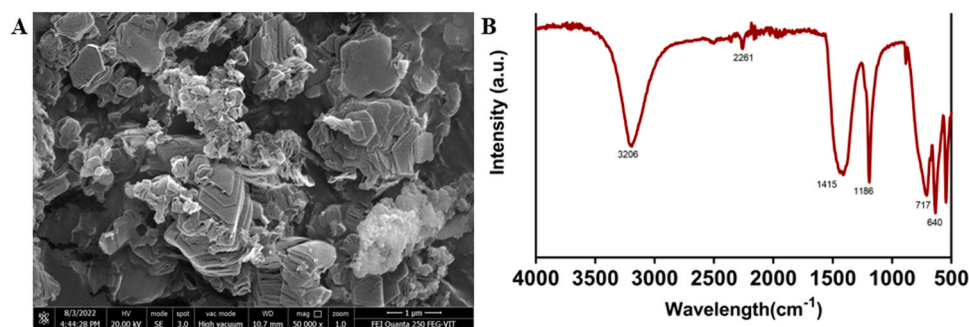


Fig. 1. Characterization of nanoparticles (A) FE-SEM pictures of boron nitride nanoparticles (BNNPs) and (B) FTIR spectra of BNNPs.

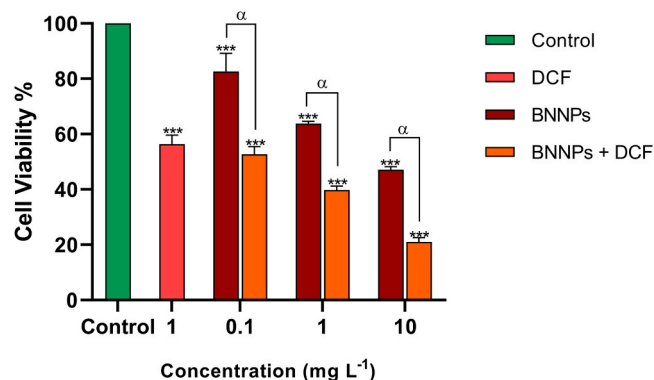


Fig. 2. Comparison of cell viability of *Scenedesmus obliquus* cells treated with pristine DCF, pristine BNNPs and their binary combinations. The level of significance in comparison to the control was represented by “\*\*\*” and “ $\alpha$ ” ( $p < 0.001$ ), which showed the level of significance in comparison between pristine BNNPs and binary mixture.

significantly ( $p < 0.001$ ) compared to the control. The BNNPs + DCF treated cells showed a significant increase in ROS generation ( $p < 0.001$ ) compared to the control samples. A significant difference in ROS generation ( $p < 0.001$ ) was observed for BNNPs + DCF-treated algal cells compared to those treated with pristine BNNPs.

In Fig. 3B, superoxide radical generation revealed that, for the cells treated with pristine DCF (1 mg L<sup>-1</sup>), various concentrations (0.1, 1, 10 mg L<sup>-1</sup>) of pristine BNNPs and their binary combinations, the superoxide radical was increased significantly ( $p < 0.001$ ) compared to the control. With the increasing concentration, superoxide oxide radical generation was also significantly increased for the binary mixture treated samples compared to various concentrations of pristine BNNPs. Our data also showed a similar trend for hydroxyl radical generation (Fig. 3C). Hydroxyl radical production was significantly increased ( $p < 0.001$ ) for the mixture-treated samples compared to control and pristine BNNP-treated samples.

MDA produced in response to pristine DCF, different concentrations of pristine BNNPs, and their binary mixture are represented in Fig. 3D. In our study, MDA content was significantly increased for algal samples ( $p < 0.001$ ) treated with pristine DCF, pristine BNNPs, and their binary combinations in comparison to the control samples. The increase in MDA production for binary mixture treated samples was significant ( $p <$

0.001) compared to pristine BNNPs treated samples.

### 3.4. Antioxidant enzymatic activity

The catalase activity in all the contaminant-treated cells was significantly more ( $p < 0.001$ ) than in control cells. Fig. 4A reveals the catalase activity, and the increment observed for the binary mixture treated samples was highly significant with respect to pristine BNNPs counterparts ( $p < 0.001$ ).

A similar trend was observed for SOD as well, as represented in Fig. 4B. The results indicate that an increment in SOD activities was noted for the cells treated with pristine DCF, pristine BNNPs, and their binary mixture when compared to untreated cells ( $p < 0.001$ ). Algal cells treated with a binary mixture revealed increased SOD activity compared to algal cells treated with pristine BNNPs ( $p < 0.001$ ).

### 3.5. Photosynthetic yield parameters

Fig. 5A represents the photosynthetic efficiency of PS II ( $\Phi_m$ ) for the BNNPs. Pristine DCF and pristine BNNPs treated samples substantially reduced the  $\Phi_m$  value compared to the untreated samples. The samples treated with various concentrations of BNNPs + DCF showed a significant reduction in the  $\Phi_m$  value compared to untreated and pristine BNNPs.

Fig. 5B displayed the electron transport rate within the PS II system in the interacted cells. All the contaminant-treated samples showed a highly significant decrease in ETR with respect to the control samples. The ETR<sub>max</sub> was further reduced ( $p < 0.001$ ) when cells treated with DCF and BNNPs combinations compared to pristine BNNPs treated cells.

## 4. Discussion

The fact that the BNNPs solution has a negative zeta potential value shows that there are significant forces of repulsion between the nanoparticles. These forces prevent the nanoparticles from agglomerating, maintaining the nanoparticles' long-term stability in the colloidal suspension [45]. DCF in the system makes it even more stable, as evidenced by the zeta potential values. The mean hydrodynamic diameter of the particles increased with increasing BNNPs concentrations. The MHD of the particles increased a bit when BNNPs were combined with DCF. The interaction between the numerous organic colloidal particles in the freshwater matrix and the particles might be responsible for the growth

Table 1  
Independent action model for the mixture of BNNPs and DCF.

Concentration of DCF (mg L <sup>-1</sup> )	Concentration of BNNPs (mg L <sup>-1</sup> )	Observed toxicity (%)	Expected toxicity (%)	Ratio of Inhibition (R <sub>i</sub> )	P value	Nature of interaction
1	0.1	52.69	79.42	0.66 ± 0.04	<0.001	Antagonistic
	1	39.82	73.78	0.54 ± 0.03	<0.001	Antagonistic
	10	21.02	65.52	0.32 ± 0.02	<0.001	Antagonistic



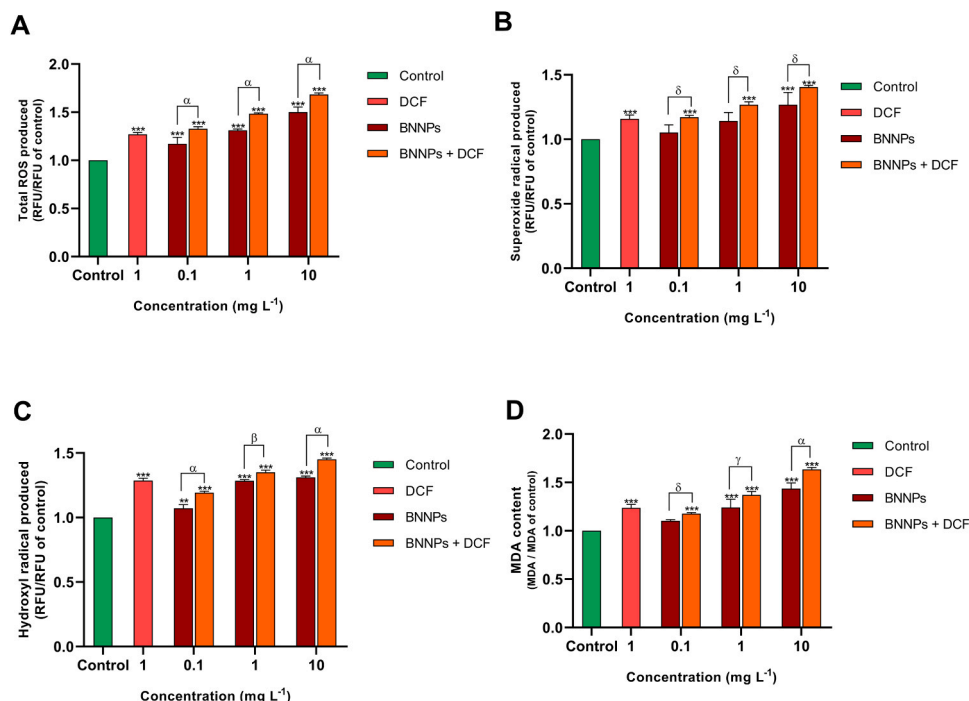


**Fig. 3.** The production of oxidative stress by nanoparticles is assessed. **(A)** Comparison of the production of total ROS, **(B)** superoxide radicals, **(C)** hydroxyl radicals, and **(D)** MDA production. The level of significance with respect to control was represented by “\*\*\*\*” ( $p < 0.001$ ), “\*\*\*” ( $p < 0.01$ ); “ $\alpha$ ” ( $p < 0.001$ ), “ $\beta$ ” ( $p < 0.01$ ), “ $\gamma$ ” ( $p < 0.05$ ), and “ $\delta$ ” ( $p > 0.05$ ) showed the level of significance in comparison between pristine BNNPs and binary mixture. The data are the averages of at least three independent experiments ( $n \geq 3$ ); the standard deviations are shown (vertical error bars). The mean values were represented using a two-way ANOVA test with a Bonferroni post-test.

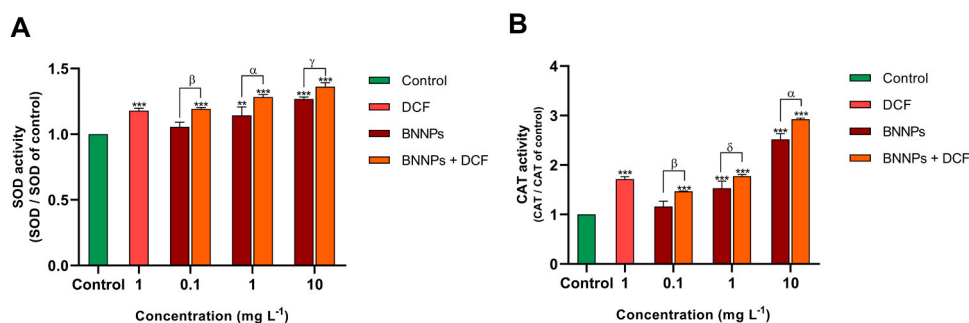


**Fig. 4.** *Scenedesmus obliquus* treated with pristine DCF, pristine BNNPs and their binary combinations produced antioxidant enzyme activity, which was measured. **(A)** A comparison of the catalase activity. **(B)** A comparison of the SOD activity. The level of significance with respect to control was represented by “\*\*\*\*” ( $p < 0.001$ ), “ $\alpha$ ” ( $p < 0.001$ ), “ $\beta$ ” ( $p < 0.01$ ), “ $\gamma$ ” ( $p < 0.05$ ), and “ $\delta$ ” ( $p > 0.05$ ) showed the level of significance in comparison between pristine BNNPs and binary mixture. The data are the averages of at least three independent experiments ( $n \geq 3$ ); the standard deviations are shown (vertical error bars). The mean values were represented using a two-way ANOVA test with a Bonferroni post-test.

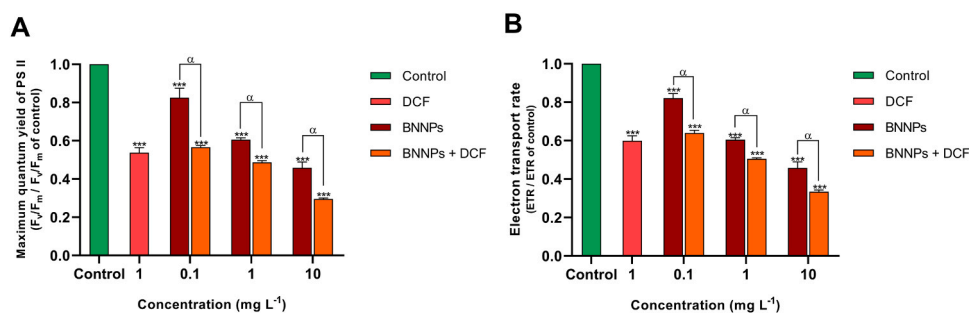


**Fig. 5.** Photosynthetic parameters in *Scenedesmus obliquus* exposed to pristine DCF, pristine BNNPs, and their binary combinations were assessed. **(A)** The comparison of maximum quantum yield of PS II ( $\Phi_m$ ) **(B)** The comparison of electron transport rate. The level of significance with respect to control was represented by “\*\*\*\*” ( $p < 0.001$ ), and “ $\alpha$ ” ( $p < 0.001$ ) showed the level of significance in comparison between pristine BNNPs and binary mixture.

in the hydrodynamic size of the particles [38].

A concentration-dependent reduction was noted in the cell viability when exposed to different concentrations of pristine BNNPs and its binary mixture. This might be due to the particle accumulation on the algal cell surface, thereby preventing other nutrients from passing into the algal cells [20]. In an earlier study, which was done by Saxena et al. [41], the exposure of boron nanoparticles at concentrations of 10, 50, and 100 mg L<sup>-1</sup> on two freshwater microalgae named *Coelastrella terrestris* and *Chlorella vulgaris* showed a similar trend of reduced cell viability. Another critical theory that might have been related to growth inhibition is reduced light availability. On increasing the concentration of NPs, the turbidity of the growth media increases, thereby reducing the light entering the cells, which was previously discussed by Choi et al. [5]. When DCF was combined with BNNPs, the reduction in cell viability further increased. DCFs might have adsorbed onto the nanoparticles, which accumulate on the algal cell surface and thus get entry into the algal cells. Previous research indicates that DCF has a significant ability to adsorb NPs by chemisorption, particularly when compared to other NSAIDs. This is attributed to the existence of an amine group plus aromatic rings in its molecular structure. The level of chemisorption is directly influenced by the amount of surface area accessible on the adsorbent. Therefore, as the specific surface area of the adsorbent increases, the sorption capacity also increases [24]. The enhanced toxicity found at high concentrations of BNNPs and DCF is attributed to the abundance of sorption sites on BNNPs, which facilitate the adsorption of DCF. Antagonistic effects have been seen for all combinations resulting from the competition of binding sites on the algal cell membrane for cellular entry.

A steady increase in oxidative stress, i.e., total ROS, specific ROS, and lipid peroxidation, was observed, with the increase in the concentration of pristine BNNPs and in combination with DCF. This represents a correlation between cytotoxicity and oxidative stress, which was concentration-dependent. The possible adsorption of BNNPs on the algal cells affects the photosynthesis and thereby, the movement of electrons from the PS II to cytochrome b6/f. This caused aggravation in the photoinhibition and an over-accumulation of radicals at that site, ultimately leading to increased oxidative stress [6]. Furthermore, BNNPs aggregation on the algal surface led to cell membrane depletion, which provides an opportunity for DCF to gain cellular entry. Current investigation showed MDA content was significantly greater in the treated cells than in untreated cells. One of the primary mechanisms underlying cytotoxicity is lipid peroxidation caused by ROS generation. As a result, the increase in MDA level could be linked to the stress caused by increased ROS formation following BNNPs treatment. A recent study by Saxena et al. [41] showed highly increased MDA content in *Chlorella vulgaris* and *Coelastrella terrestris* after treatment with different concentrations of boron nitride nanoparticles, corroborating our findings. Nonetheless, a higher level of MDA production was noticeable because nanoparticles had more surface area than volume. Studies have shown that DCF can hinder the development of different types of microalgae, interfere with cellular processes, and negatively impact the process of photosynthesis [46]. Previous research has shown that when green microalgae, such as *Chlorella vulgaris* and *Scenedesmus obliquus*, are exposed to DCF, their chlorophyll content and photosynthetic efficiency decrease. In addition, DCF-induced oxidative stress leads to excessive generation of ROS, which in turn causes lipid peroxidation, protein oxidation, and DNA damage in algal cells. Elevated levels of ROS also stimulate the initiation of antioxidant defense mechanisms, such as the enhancement of enzymes like CAT and SOD [16]. The findings showed that ROS-mediated oxidative stress stimulates cellular stress responses and defense systems.

Since antioxidant enzymes like catalase and superoxide dismutase support cells by lowering intracellular ROS levels, their activity can be used as oxidative stress markers. These enzymes alleviate oxidative stress by converting harmful cellular peroxides like free radical O<sub>2</sub> and H<sub>2</sub>O<sub>2</sub> to nontoxic O<sub>2</sub> and H<sub>2</sub>O [23]. The increased concentration of

BNNPs and DCF induced more oxidative radicals, affecting the membrane damage and thus causing more MDA production [4]. Furthermore, the uptake of foreign chemicals, such as pharmaceuticals, causes intracellular ROS production in microalgae [21,22]. The cell's toxicity can be related to oxidative stress and nanoparticle aggregation on the algal cells' surface, affecting the algal cells' photosynthetic function. Previous studies from our lab showed increased antioxidant activities of marine algal cells *Chlorella sp.* when treated with nanoTiO<sub>2</sub> and tetracycline, corroborating our findings [42].

The modification of the balance between both the electron transfer rate and the excitation energy demonstrates that the loss of light energy to heat can reduce total photosynthetic performance. Giri and Mukherjee [15] previously showed that as the quantity of pollutants increases, the Fv/Fm ratio drops, increasing the harmful effects on algal photosynthetic efficiency (PS II). In the present study, the pure BNNPs and BNNPs + DCF treated samples likewise had very low Fv/Fm values, indicating severe impairment to the PS II system. Additionally, electron transport rate, another photosynthetic measure, followed a similar pattern. It is possible that the electron transport rate across the PS II system was reduced under stress from both BNNPs and DCF. This resulted in a significant build-up of electrons, intensifying photo inhibition and increasing ROS. The high concentration of ROS species in the cells caused cell structure damage and prevented chlorophyll synthesis, substantially reducing photosynthetic yield and thereby increasing toxicity. A possible cause is the presence of boron nitride on the surface of algal cells, which reduces the amount of light available to algal cells [27]. Reduced light accessibility lowered growth and produced stress, decreasing photosynthetic yield and electron transport rate. Similar results were reported in the prior investigation conducted by Saxena et al. [41]. They discovered that chlorophyll and carotenoid content decreased when the concentration of boron nitride nanoparticles increased. Another potential scenario is that DCF infiltrated the algal cells and caused damage to the photosynthetic centers. Moreover, the combination of BNNPs and DCF increased oxidative stress, resulting in a decrease in photosynthetic activities. A similar study by Christudoss et al. [7] showed that increased DCF concentrations impaired photosynthetic parameters in *Scenedesmus obliquus*, thus reducing photosynthetic activities.

An analysis was conducted using a heat map (Fig. 6) to examine the connections between different toxicity indicators in varying exposure conditions. There was a clear link between the rise in ROS levels, MDA production, and the increment in CAT activity. This suggests that the

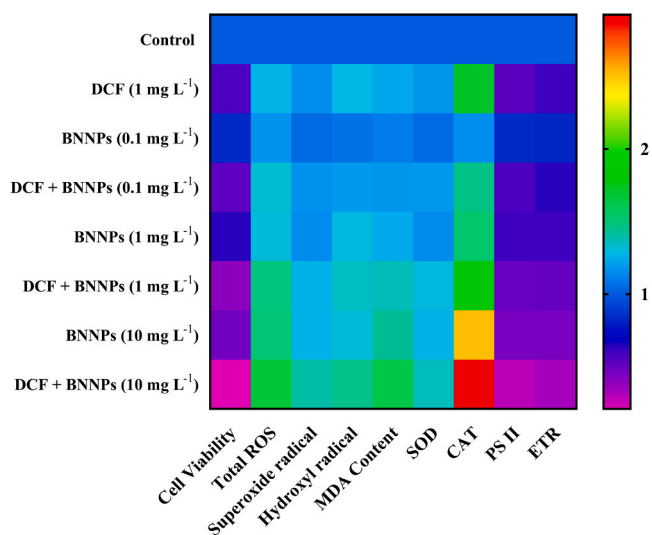


Fig. 6. : Heat map representation of the effects of various concentrations of pristine DCF, pristine BNNPs, and their binary combinations on the various biochemical activities of *Scenedesmus obliquus* after 72 h of exposure.

cells activated antioxidant enzymes to better handle the build-up of ROS within the cell. In addition, there was a notable correlation between the enhancement in oxidative stress and the decrease in photosynthetic activities.

## 5. Conclusions

The present work demonstrates that when *Scenedesmus obliquus* was exposed to BNNPs and DCF combined, it decreased cell viability with increasing cellular oxidative stress and antioxidant defense mechanisms. Excessive ROS generation generally impairs the cell's capacity to operate by reducing photosynthesis and electron transport in the cells. These nanomaterials are among the most hazardous freshwater contaminants, so the present research results are noteworthy. Future studies employing diverse model organisms should provide insight into the potential effects of different nanoparticle combinations in freshwater environments.

## CRedit authorship contribution statement

**Soupam Das:** Writing – original draft, Validation, Methodology, Investigation, Conceptualization. **Shinta Ann Jose:** Methodology, Investigation. **Sampriti Giri:** Methodology, Investigation. **Janmey Shah:** Methodology, Investigation. **Mrudula Pulimi:** Writing – review & editing, Formal analysis, Conceptualization. **Shalini Anand:** Writing – review & editing, Formal analysis. **Pramod Kumar Rai:** Writing – review & editing, Project administration, Funding acquisition. **AMITAVA MUKHERJEE:** Writing – review & editing, Validation, Supervision, Resources, Project administration, Funding acquisition, Formal analysis, Conceptualization.

## Declaration of Competing Interest

The authors declare that they have no known competing financial interests or personal relationships that could have appeared to influence the work reported in this paper.

## Data Availability

Data will be made available on request.

## Acknowledgements

The authors thank the Vellore Institute of Technology, Vellore, for providing this study's FE-SEM and XRD facilities. The authors would also like to express sincere gratitude to Sh. Rajiv Narang (Outstanding Scientist and Director), Centre for Fire, Explosives, and Environment Safety - Defence Research and Development Organisation (CFEES-DRDO). The study was performed with the help of funding provided by CFEES-DRDO (Sanction No. CFEES/TCP/EnSG/CARS(P)/DG(SAM)/FTS-ERAF/VIT-VELLORE).

## Appendix A. Supporting information

Supplementary data associated with this article can be found in the online version at [doi:10.1016/j.toxrep.2024.101696](https://doi.org/10.1016/j.toxrep.2024.101696).

## References

- J.M. Angosto, M.J. Roca, J.A. Fernández-López, Removal of diclofenac in wastewater using biosorption and advanced oxidation techniques: comparative results, *Water* 12 (2020) 3567.
- S. Bao, X. Nie, Y. Liu, C. Wang, W. Li, S. Liu, Diclofenac exposure alter the expression of PXR and its downstream target genes in mosquito fish (*Gambusia affinis*), *Sci. Total Environ.* 616 (2018) 583–593.
- D. Chakraborty, K. Ethiraj, N. Chandrasekaran, A. Mukherjee, Mitigating the toxic effects of CdSe quantum dots towards freshwater alga *Scenedesmus obliquus*: role of eco-corona, *Environ. Pollut.* 270 (2021) 116049.
- F. Chen, Z. Xiao, L. Yue, J. Wang, Y. Feng, X. Zhu, Z. Wang, B. Xing, Algae response to engineered nanoparticles: current understanding, mechanisms and implications, *Environ. Sci.: Nano* 6 (2019) 1026–1042.
- M.-H. Choi, Y. Hwang, H.U. Lee, B. Kim, G.-W. Lee, Y.-K. Oh, H.R. Andersen, Y.-C. Lee, Y.S. Huh, Aquatic ecotoxicity effect of engineered aminoclay nanoparticles, *Ecotoxicol. Environ. Saf.* 102 (2014) 34–41.
- M. Choudhary, U.K. Jetley, M.A. Khan, S. Zutshi, T. Fatma, Effect of heavy metal stress on proline, malondialdehyde, and superoxide dismutase activity in the cyanobacterium *Spirulina platensis*-S5, *Ecotoxicol. Environ. Saf.* 66 (2007) 204–209.
- A.C. Christudoss, N. Chandrasekaran, A. Mukherjee, Polystyrene nanoplastics alter the ecotoxicological effects of diclofenac on freshwater microalgae *Scenedesmus obliquus*, *Environ. Sci.: Process. Impacts* 26 (2024) 56–70.
- M. Cleuvers, Mixture toxicity of the anti-inflammatory drugs diclofenac, ibuprofen, naproxen, and acetylsalicylic acid, *Ecotoxicol. Environ. Saf.* 59 (2004) 309–315.
- Y. Dağlıoğlu, B.Y. Öztürk, A comparison of the acute toxicity and bioaccumulation of boron particles (nano and micro) in *Chodatodesmus mucronulatus*, *J. Boron* 3 (2018) 157–165.
- S. Das, N. Chandrasekaran, A. Mukherjee, Unmasking effects of masks: Microplastics released from disposable surgical face masks induce toxic effects in microalgae *Scenedesmus obliquus* and *Chlorella* sp., *Comp. Biochem. Physiol. Part C: Toxicol. Pharmacol.* (2023) 109587.
- S. Das, S. Giri, G. Wadhwa, M. Pulimi, S. Anand, N. Chandrasekaran, S.A. Johari, P. K. Rai, A. Mukherjee, Comparative ecotoxicity of graphene, functionalized multi-walled CNTs, and their mixture in freshwater microalgae, *Scenedesmus obliquus*: analyzing the role of oxidative stress, *Environ. Sci. Pollut. Res.* 30 (2023) 70246–70259.
- S. Das, A. Mukherjee, Combined effects of P25 TiO<sub>2</sub> nanoparticles and disposable face mask leachate on microalgae *Scenedesmus obliquus*: analysing the effects of heavy metals, *Environ. Sci.: Process. Impacts* 25 (2023) 1428–1437.
- S. Das, V. Thiagarajan, N. Chandrasekaran, B. Ravindran, A. Mukherjee, Nanoplastics enhance the toxic effects of titanium dioxide nanoparticle in freshwater alga *Scenedesmus obliquus*, *Comp. Biochem. Physiol. Part C: Toxicol. Pharmacol.* 256 (2022) 109305.
- H. Dolezalová Weissmannová, J. Pavlovský, L. Fišerová, H. Kosárová, Toxicity of diclofenac: cadmium binary mixtures to algae *Desmodesmus subspicatus* using normalization method, *Bull. Environ. Contam. Toxicol.* 101 (2018) 205–213.
- S. Giri, A. Mukherjee, Ageing with algal EPS reduces the toxic effects of polystyrene nanoplastics in freshwater microalgae *Scenedesmus obliquus*, *J. Environ. Chem. Eng.* 9 (2021) 105978.
- M. González-Pleiter, S. Gonzalo, I. Rodea-Palomares, F. Leganés, R. Rosal, K. Boltes, E. Marco, F. Fernández-Piñas, Toxicity of five antibiotics and their mixtures towards photosynthetic aquatic organisms: implications for environmental risk assessment, *Water Res.* 47 (2013) 2050–2064.
- K. Górnik, L.B. Lahuta, Application of phytohormones during seed hydropriming and heat shock treatment on sunflower (*Helianthus annuus* L.) chilling resistance and changes in soluble carbohydrates, *Acta Physiol. Plant.* 39 (2017) 1–12.
- I.C. Guiloski, L.D.S. Piancini, A.C. Dagostim, S.L. de Moraes Calado, L.F. Fávaro, S. L. Boschen, M.M. Cestari, C. da Cunha, H.C.S. de Assis, Effects of environmentally relevant concentrations of the anti-inflammatory drug diclofenac in freshwater fish *Rhamdia quelen*, *Ecotoxicol. Environ. Saf.* 139 (2017) 291–300.
- A. Hayat, M. Sohail, M.S. Hamdy, T. Taha, H.S. AlSalem, A.M. Alenad, M.A. Amin, R. Shah, A. Palamanit, J. Khan, Fabrication, characteristics, and applications of boron nitride and their composite nanomaterials, *Surf. Interfaces* 29 (2022) 101725.
- R. Hjorth, S.N. Sørensen, M.E. Olsson, A. Baun, N.B. Hartmann, A certain shade of green: can algal pigments reveal shading effects of nanoparticles? *Integr. Environ. Assess. Manag.* 12 (2016).
- J.Y. Kim, C.R. Jin, H.S. Kim, J. Park, Y.-E. Choi, Fluorogenic “on-off” nanosensor based on dual-quenching effect for imaging intracellular metabolite of various microalgae, *Biosens. Bioelectron.* 198 (2022) 113839.
- J.Y. Kim, C.R. Jin, J. Park, D.G. Kim, H.S. Kim, Y.-E. Choi, Simultaneous probing of dual intracellular metabolites (ATP and paramylon) in live microalgae using graphene oxide/aptamer nanocomplex, *Microchim. Acta* 189 (2022) 88.
- K.Y. Kim, S.M. Kim, J.Y. Kim, Y.-E. Choi, Elucidating the mechanisms underlying the cytotoxic effects of nano-/micro-sized graphene oxide on the microalgae by comparing the physiological and morphological changes in different trophic modes, *Chemosphere* 309 (2022) 136539.
- J. Li, X. Huang, Z. Hou, T. Ding, Sorption of diclofenac by polystyrene microplastics: kinetics, isotherms and particle size effects, *Chemosphere* 290 (2022) 133311.
- M. Li, G. Huang, X. Chen, J. Yin, P. Zhang, Y. Yao, J. Shen, Y. Wu, J. Huang, Perspectives on environmental applications of hexagonal boron nitride nanomaterials, *Nano Today* 44 (2022) 101486.
- Y. Liu, L. Wang, B. Pan, C. Wang, S. Bao, X. Nie, Toxic effects of diclofenac on life history parameters and the expression of detoxification-related genes in *Daphnia magna*, *Aquat. Toxicol.* 183 (2017) 104–113.
- D. Metzler, A. Erdem, Y. Tseng, C. Huang, Responses of algal cells to engineered nanoparticles measured as algal cell population, chlorophyll a, and lipid peroxidation: effect of particle size and type, *J. Nanotechnol.* 2012 (2012).
- L. Natarajan, D. Soupam, S. Dey, N. Chandrasekaran, R. Kundu, S. Paul, A. Mukherjee, Toxicity of polystyrene microplastics in freshwater algae *Scenedesmus obliquus*: effects of particle size and surface charge, *Toxicol. Rep.* 9 (2022) 1953–1961.
- OECD, 202: *Daphnia* sp. acute immobilisation test, OECD Guidel. Test. Chem. 6 (2004). Sections 2.

- [30] E. Owusu-Ansah, A. Yavari, U. Banerjee, A protocol for in vivo detection of reactive oxygen species, *Protoc. Exch.* (2008).
- [31] P.K. Pandey, M.N. Ajima, K. Kumar, N. Poojary, S. Kumar, Evaluation of DNA damage and physiological responses in Nile tilapia, *Oreochromis niloticus* (Linnaeus, 1758) exposed to sub-lethal diclofenac (DCF), *Aquat. Toxicol.* 186 (2017) 205–214.
- [32] M. Parolini, A. Binelli, D. Cogni, C. Riva, A. Provini, An in vitro biomarker approach for the evaluation of the ecotoxicity of non-steroidal anti-inflammatory drugs (NSAIDs), *Toxicol. Vitro.* 23 (2009) 935–942.
- [33] A. Piotrowska-Niczyporuk, A. Bajguz, E. Zambrzycka, B. Godlewska-Zylkiewicz, Phytohormones as regulators of heavy metal biosorption and toxicity in green alga *Chlorella vulgaris* (Chlorophyceae), *Plant Physiol. Biochem.* 52 (2012) 52–65.
- [34] A.G. Rickard, M. Zhuang, C.A. DeRosa, X. Zhang, M.W. Dewhirst, C.L. Fraser, G. M. Palmer, Dual-emissive, oxygen-sensing boron nanoparticles quantify oxygen consumption rate in breast cancer cells, *J. Biomed. Opt.* 25 (2020) 116504, 116504.
- [35] Z. Romanowska-Duda, M. Grzesik, R. Janas, Maximal efficiency of PSII as a marker of sorghum development fertilized with waste from a biomass biodegradation to methane, *Front. Plant Sci.* 9 (2019) 1920.
- [36] B. Roy, H. Chandrasekaran, S.P. Krishnan, N. Chandrasekaran, A. Mukherjee, UVA pre-irradiation to P25 titanium dioxide nanoparticles enhanced its toxicity towards freshwater algae *Scenedesmus obliquus*, *Environ. Sci. Pollut. Res.* 25 (2018) 16729–16742.
- [37] B. Roy, P. Suresh, N. Chandrasekaran, A. Mukherjee, UVB pre-irradiation of titanium dioxide nanoparticles is more detrimental to freshwater algae than UVA pre-irradiation, *J. Environ. Chem. Eng.* 8 (2020) 104076.
- [38] R. Roy, A. Parashar, M. Bhuvaneshwari, N. Chandrasekaran, A. Mukherjee, Differential effects of P25 TiO<sub>2</sub> nanoparticles on freshwater green microalgae: *Chlorella* and *Scenedesmus* species, *Aquat. Toxicol.* 176 (2016) 161–171.
- [39] C. Russo, R. Nugnes, E. Orlo, A. di Matteo, B. De Felice, C. Montanino, M. Lavorgna, M. Isidori, Diclofenac eco-geno-toxicity in freshwater algae, rotifers and crustaceans, *Environ. Pollut.* 335 (2023) 122251.
- [40] P. Sathishkumar, R.A.A. Meena, T. Palanisami, V. Ashokkumar, T. Palvannan, F. L. Gu, Occurrence, interactive effects and ecological risk of diclofenac in environmental compartments and biota—a review, *Sci. Total Environ.* 698 (2020) 134057.
- [41] P. Saxena, A.K. Gupta, V. Saharan, Harish, Toxicity of boron nitride nanoparticles influencing bio-physicochemical responses in freshwater green algae, *Environ. Sci. Pollut. Res.* 30 (2023) 23646–23654.
- [42] V. Thiagarajan, L. Natarajan, R. Seenivasan, N. Chandrasekaran, A. Mukherjee, Tetracycline affects the toxicity of P25 n-TiO<sub>2</sub> towards marine microalgae *Chlorella* sp., *Environ. Res.* 179 (2019) 108808.
- [43] C. Trombini, M. Hampel, J. Blasco, Assessing the effect of human pharmaceuticals (carbamazepine, diclofenac and ibuprofen) on the marine clam *Ruditapes philippinarum*: An integrative and multibiomarker approach, *Aquat. Toxicol.* 208 (2019) 146–156.
- [44] D. Wojcieszynska, H. Guzik, U. Guzik, Non-steroidal anti-inflammatory drugs in the era of the Covid-19 pandemic in the context of the human and the environment, *Sci. Total Environ.* 834 (2022) 155317.
- [45] J. Yin, G. Huang, C. An, R. Feng, Nanocellulose enhances the dispersion and toxicity of ZnO NPs to green algae *Eremosphaera viridis*, *Environ. Sci.: Nano* 9 (2022) 393–405.
- [46] Y. Zhang, S.-U. Geißen, C. Gal, Carbamazepine and diclofenac: removal in wastewater treatment plants and occurrence in water bodies, *Chemosphere* 73 (2008) 1151–1161.
- [47] Y. Zhu, P. Prommana, N.S. Hosmane, P. Coghi, C. Uthaipibull, Y. Zhang, Functionalized boron nanoparticles as potential promising antimalarial agents, *ACS Omega* 7 (2022) 5864–5869.